# Enhanced Biocompatibility and Biostability of CdTe Quantum Dots by Facile Surface-Initiated Dendritic Polymerization

Li Zhou,[†,‡] Chao Gao,[*,†] Weijian Xu,[*,‡] Xue Wang,[§] and Yuhong Xu[*,§]

*Key Laboratory of Macromolecular Synthesis and Functionalization (Ministry of Education), Department of Polymer Science and Engineering, Zhejiang University, 38 Zheda Road, Hangzhou 310027, People's Republic of China, Institute of Polymer Science and Engineering, College of Chemistry and Chemical Engineering, Hunan University, Changsha 410082, People's Republic of China, and School of Pharmacy, Shanghai Jiao Tong University, 800 Dongchuan Road, Shanghai 200240, People's Republic of China*

*Received March 9, 2009; Revised Manuscript Received May 17, 2009*

The synthesis of stable, low toxic, multifunctional, and water-soluble quantum dots (QDs) is of crucial importance for nanobiotechnology. An in situ anionic ring-opening polymerization strategy was successfully employed to grow multihydroxyl hyperbranched polyglycerol (HPG) from surfaces of aqueous synthesized QDs directly, affording multifunctional CdTe@HPG nanohybrids. The grafted HPG content can be adjusted from about 25 to 80 wt % by manipulating the feed ratio of glycidol monomer to QDs. The resultant CdTe@HPGs still show strong fluorescence and well water-solubility, and can conjugate functional biomolecules (e.g., amino acids) with their multiple reactive hydroxyls. Cytotoxicity measurements reveal that the CdTe@HPGs are much less toxic than the pristine QDs in human lung cancer cells SPCAI and more grafted HPG leads to less toxicity, due to the envelope of biocompatible HPG on QDs. It was found that the pristine QDs were unstable and their fluorescence decreased greatly or was even completed quenched after 24 h in SPCAI cells, whereas the QD@HPGs still exhibited strong fluorescence. This report opens the door for using in situ controlled/living polymerization to tailor QDs with biocompatible dendritic polymers readily and casts a light for obtaining robust nontoxic functionalized QDs and applying them in vitro and in vivo.

## Introduction

In recent decades, quantum dots (QDs, also know as semiconductor nanocrystals) have received wide interest for application in optical devices, solar cells, biological imaging, and diagnostics due to their unique physical and chemical properties.[1−6] Compared with organic fluorophores, QDs exhibit unique size-dependent optical and electronic properties, narrow emission spectra, broad absorption spectra, and good photostability. Generally, QDs are synthesized via two strategies: organic phase and aqueous phase. The organic phase method can give birth to high quality QDs with well-crystalline structure and high photoluminescent quantum yield (QY, 40−80%).[7] However, these QDs are not water-soluble due to their surface coated with a hydrophobic layer such as trioctylphosphine (TOP) and trioctylphosphine oxide (TOPO), and thus, they cannot be directly used in biological environments. Usually, a ligand exchange strategy is required to substitute hydrophilic molecules such as phospholipids, thiol-molecules, and amphiphilic polymer for TOPO molecules.[8] The exchange process is complicated and often leads to a significant decrease in QY of the QDs or even the fluorescence is absolutely quenched.[9] Additionally, because the TOPO molecules cannot be completely replaced by just one exchange process, these QDs are not stable enough in aqueous solution after ligand exchange.[10] Alternatively, water-soluble QDs can be directly synthesized via an aqueous phase method.[11,12] In contrast to the organic phase method, aqueous phase synthesis is simpler and cheaper, and especially, the products prepared in the aqueous phase have excellent water solubility and biocompatibility. However, QDs synthesized in aqueous phase usually show low QY (lower 10%). Recently, the QY of the QDs were enhanced to 40−70% by optimization of the aqueous synthesis condition and application of novel reactor such as microwave and autoclave.[13,14] Thus, the aqueous synthesized QDs become attractive in biological research.

Nevertheless, for biological applications, it should be noted that the small thiol-molecules ligand cannot totally enwrap the QDs. The $Cd^{2+}$ ions can release from the QDs especially under UV irradiation, thereby making QDs toxic to the biosystem.[15] Therefore, it is necessary to protect the QD surfaces to improve their biocompatibility. One of such strategies is to coat QDs with inorganic shell, forming core−shell (e.g., CdSe/ZnS,[16] CdTe/CdSe[17] and CdTe/$SiO_2$[18]) or core−shell−shell structures (e.g., CdSe/CdS/ZnS[19]). Although the biocompatibility and QY of the QDs were highly improved by this strategy, their surface functional groups for further modification are awfully lacking. Another effective strategy is to coat QDs with polymer. On one hand, the polymer can improve the surface stability of QDs, which directly affects the fluorescence intensity and toxicity; on the other hand, polymer endows QDs with new physical and chemical properties including solubility, processability, chemical and biological stability, biocompatibility, and further functionalization possibility. In this regard, two main methodologies have been developed to prepare QD-polymer nanohybrids (QD@polymer): "polymer first" and "QDs first" approaches. The former involves first synthesis of functional polymer, and then utilizes the functional polymer as template

* To whom correspondence should be addressed. E-mail: chaogao@zju.edu.cn (C.G.); weijxu@hnu.cn (W.X.); yhxu@sjtu.edu.cn (Y.X.).
† Zhejiang University.
‡ Hunan University.
§ Shanghai Jiao Tong University.

10.1021/bm9002877 CCC: $40.75 © 2009 American Chemical Society
Published on Web 06/04/2009

or ligand to grow QDs. This approach is easy to carry out with many end-capped or modified polymers such as hyperbranched polyglycerol,[20] polyamidoamine (PAMAM) dendrimer,[21] and polystyrene-poly(acrylic acid) (PS-PAA) copolymer.[22] However, the intensity of fluorescence or QY value of the products by this approach is relatively low. The "QDs first" route involves first synthesis of QDs, and subsequently utilizes the QDs as substrates to graft polymer. Thus, ligand exchange, ligand capping, and directly in situ polymerization approaches have been tried to graft various polymers such as PS,[23] poly(methyl methacrylate) (PMMA),[24] poly(caprolactone) (PCL),[25] polyacrylamide (PAM),[26] poly(maleic anhydride-alt-1-octadecene)-poly(ethylene glycol) (PMAO-PEG) copolymer,[27] polyurethane (PU),[28] poly(*N*-isopropylacrylamide) (PNIPAM),[29] poly(3-hexylthiophene),[30] as well as dendritic PAMAM,[31] onto the surfaces of QDs.

Although many concerns have been focused on the synthesis of QD@polymer *via* the "QDs first" methodology, however, controlled/living polymerization techniques as a very effective strategy to grow polymer from surfaces of inorganic nanoparticles such as Au,[32] $SiO_2$,[33] $C_{60}$,[34] and magnetic nanoparticles[35] with controllable, designable, and tailored feasible structures are still studied limitedly on QDs because the QDs are susceptible to external environment and easy to lose their fluorescence during the reaction. Emrick and co-workers pioneered in the preparation of QDs@polymer hybrids by in situ reversible addition−fragmentation chain-transfer (RAFT) polymerization,[36] ring-opening metathesis polymerization (ROMP),[37] and nitroxide-mediated radical polymerization (NMRP)[38] based on the QDs surface functional ligand, which was presynthesized and then substituted the original ligand (e.g., TOPO) on the surface of as-prepared CdSe QDs by ligand exchange method. Similarly, Barros-Timmons and co-workers first prepared a ligand possessing chlorine-based atom transfer radical polymerization (ATRP) initiator, subsequently coated on the CdS QDs surface through ligand exchange with TOPO, and finally performed ATRP successfully.[39] It is a pity that the fluorescence information of the nanohybrids was not reported in the paper. Carrot et al. reported the synthesis of PCL functionalized CdS by directly surface-initiated ring-opening polymerization (ROP) based on the aqueous synthesized CdS,[40] whereas the fluorescent property of the PCL-grafted CdS was also not shown. We carried out the same reaction on CdTe QDs and found that the QDs lost their fluorescence after ROP likely because the catalyst can destroy the QDs structure. In short, the reported approaches to functionalize QDs are either too complicated to carry out readily (e.g., ligand exchange on the QDs obtained in oil-medium) or easy to lose the optical property of QDs during the polymerization. Besides, no or rare functional groups can be available for further modification on the QD@polymer. Importantly, none of the water-soluble QD-polymer with stable fluorescence and biocompatibility was synthesized yet. Therefore, exploring a facile and economical strategy based on the in situ polymerization to prepare QD@polymer with well water-solubility, stable optical performance, controllable structure, and multiple functional groups is fairly exigent.

To meet such a big challenge, this paper presented a novel strategy based on in situ anionic ROP to grow multihydroxyl dendritic /hyperbranched polyglycerol (HPG) from the surface of CdTe QDs, which were directly prepared in aqueous solution by thiol-chemistry (see Scheme 1). Our strategy was designed preferentially according to the following considerations: (1) good controllability of living anionic polymerization and simple process of ROP initiated with hydroxyl groups, which results in the control over grafted polymer quantity and structure, high reproducibility, and large-scale availability of products; (2) good biocompatibility and high water-solubility of polyglycerol,[41] which may decrease the toxicity of QDs and promises the bioapplications of QD@HPG; (3) multifunctional groups associated with dendritic polymer, which allows further immobilization of biomolecules on QD@polymer; and (4) water-phase synthesized QDs with surface hydroxyl groups, which makes the whole functionalization process facile, green, and cost-effective. Significantly, the optical property of the CdTe QDs is still retained after reaction. To the best of our knowledge, this is the first example to directly graft biocompatible dendritic polymer from water-soluble QDs surface by surface-initiated polymerization. It is expected that the growth of HPG on QDs surface not only considerably improves the biostability and biocompatibility of QDs but also retains the functionality of the multiple hydroxyls of HPG, which is a versatile platform for further conjugation of drugs and functional biomolecules such as proteins and amino acids.

## Experimental Section

**Materials.** Tellurium powder (Te, 99.8%), $CdCl_2$ (99+%), sodium borohydride ($NaBH_4$, 96%), 1-thioglycerol (TG, 90+%), potassium methylate solution in methanol ($CH_3OK$, 25%), and glycidol (96%) were purchased from Aldrich and used as received. BOC-L-phenylalanine (Boc-Phe-OH) was purchased from GL Biochem Ltd. (Shanghai, China). Human malignant melanoma cells A375 and human lung cancer cells SPCAI were supplied by institute of biochemistry and cell biology, Chinese Academy of Sciences (Shanghai, China). Dioxane and methanol (Shanghai Chemical Reagent. Co., Ltd., Shanghai, China) were freshly distilled before each polymerization. The other reagents were used as received without further purification.

**Characterization.** Thermogravimetric analysis (TGA) was carried on a Perkin-Elmer (PE) TGA-7 instrument with a heating rate of 20 °C $min^{-1}$ in a nitrogen flow (20 mL $min^{-1}$). Absorption and fluorescence spectra were recorded at room temperature on a PE Lambda 20 UV−visible spectrometer and Varian Cary Fluorescence spectrometer, respectively. FT-IR spectra were recorded using a PE Paragon 1000 spectrometer (KBr disk). $^1H$ NMR and $^{13}C$ inverse-gated NMR spectra were measured with a Varian Mercury Plus 400 MHz spectrometer using $D_2O$ as the solvent. Molecular weights measurements were carried out in a PE series 200 gel permeation chromatograph (GPC) with polystyrene (PS) as the standard, using DMF as the eluent at a flow rate of 1 mL/min. Transmission electron microscopy (TEM) studies were performed on a JEOL JEL2010 electron microscope at 200 kV. Scanning electron microscopy (SEM) images were recorded using FEI SIRION 200 field-emission microscope. Atomic force microscopy (AFM) was measured by Digital Instrument Nanoscape IIIa SPM, operating at the tapping mode. The dynamic light scattering (DLS) measurements were conducted using a Brookhaven particle size and zeta potential analyzer at room temperature. Fluorescence microscopy images were obtained with an IX-71 inverted fluorescence microscope (Olympus). Light emitted from a continuous wave Ar ion laser (488 nm, 10mW, Melles Griot) passing through an objective lens used to excite the samples. Confocal microscopy images were obtained with Zeiss LSM-510 confocal laser-scanning microscope using a laser at 405 nm.

**Large-Scale Preparation of Water-Soluble CdTe Quantum Dots (QDs).** Water-soluble CdTe QDs are prepared according to the protocol of literature with minor revisions.[42] In a typical procedure, 800 mg of $NaBH_4$ was transferred to a small flask, then 6.5 mL of ultrapure water was added. After 920 mg (7.21 mmol) of tellurium powder was added, the reacting flask was cooled by ice. During the reaction, a small outlet connected to the flask was kept open to discharge the pressure from the resulting hydrogen. After several hours, the black tellurium powder disappeared and white sodium tetraborate precipitate

**Scheme 1.** Preparation of QD@HPG by In Situ Ring-Opening Polymerization and Further Functionalization of the QD@HPG with Protected Amino Acid (Boc-Phe-OH)

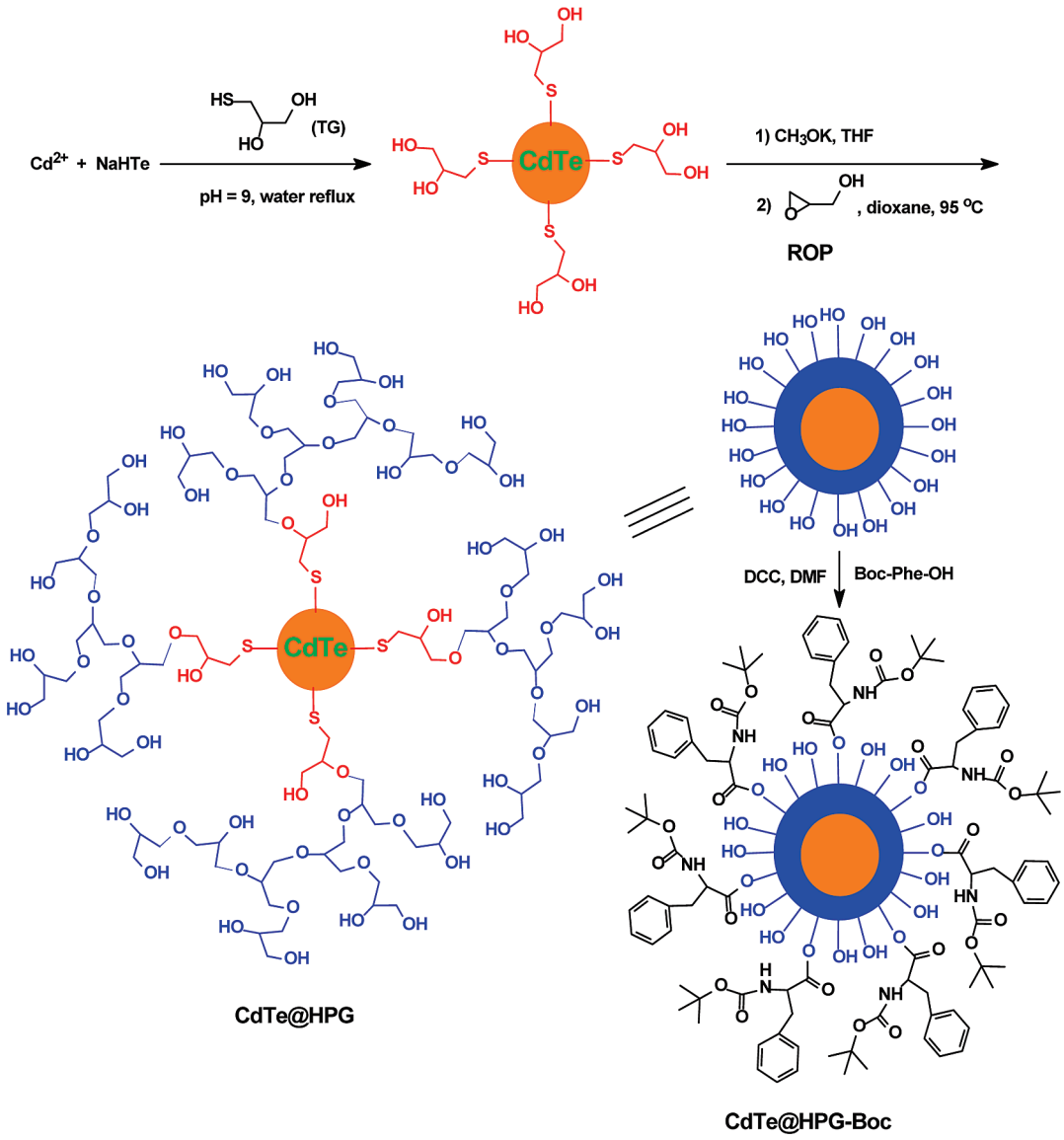


appeared on the bottom of the flask instead. The resulting fresh oxygen-free NaHTe aqueous solution was added to 1.5 L of $N_2$-saturated $CdCl_2$ solution (8.0 mM) at pH 9.0, adjusted by NaOH (1.0 M) in the presence of TG (2.8 mL, 32.33 mmol) at 100 °C. Then the mixture was refluxed for 12 h to obtain CdTe QDs with orange color. The CdTe QDs were precipitated by acetone and centrifuged, then redispersed in acetone by stirring and centrifuged. This purification cycle was repeated thrice. After purification, the resulting orange solid was dried at 60 °C for 24 h in vacuum, obtaining pristine CdTe QDs (2.06 g, $QY_{rh} = 16.8\%$ with rhodamine 6G as the reference).

**Preparation of Hyperbranched Polyglycerol-Grafted CdTe Quantum Dots.** To prepare QD@HPG nanohybrids, typically (e.g., QD@HPG1) 75 mg CdTe QDs were mixed with 20 $\mu$L (0.067 mmol) of potassium methylate ($CH_3OK$) solution in methanol (25 wt %) and 2 mL of anhydrous tetrahydrofuran (THF) in a flask. The mixture was stirred for 30 min, before which excess methanol was removed by vacuum. Then 10 mL of anhydrous dioxane was added and the flask was kept in an oil bath at 95 °C. Glycidol (500 mg, 6.76 mmol) was added dropwise over a period of 6 h. After completion of monomer addition, the mixture was stirred for an additional 1 h. The mixture was quenched and dispersed in methanol and, subsequently, centrifuged and washed several times with methanol. After repeated washing and centrifugation steps, the resulting solid was dried overnight in a vacuum, yielding QD@HPG1 (95.5 mg). Because glycidol can be self-initiated to generate HPG simultaneously, we also collected the free polymer by precipitation of the upper centrifugal solution with acetone.

**Preparation of Boc-Phe-OH-modified QD@HPG.** Typically, 100 mg (0.38 mmol) of BOC-L-phenylalanine (Boc-Phe-OH) was mixed with 5 mL of *N*,*N*-dimethylformamide (DMF) solution containing the dicyclohexylcarbodiimide (DCC, 80 mg, 0.39 mmol) and 4-(dimethylamino) pyridine (DMAP, 45 mg, 0.37 mmol). The QD@HPG3 (80 mg) was then added to the mixture at room temperature under magnetic stirring for 1 h. After removing the insoluble dicyclohexylurea by centrifugation, the resulting sample (designated as QD@HPG-Boc, in the centrifugal liquid) was precipitated by ether and dried under vacuum for 12 h at room temperature. Finally, 106.4 mg of QD@HPG-Boc was obtained.

**Cellular Cytotoxicity Evaluation.** The cytotoxicity of the pristine QDs and QD@HPG (series) were measured by MTT assay. Human lung cancer cells SPCAI were seeded in 96-well microplate at a density of approximately $1 \times 10^4$ cells per well with medium containing different concentration of pristine QDs and QD@HPG (series) for 24 h at 37 °C and 5% of $CO_2$. Then, 20 $\mu$L of MTT solution (5 mg/mL in phosphate buffer solution, pH 7.4) was added to each well followed by incubation for 4 h at 37 °C. Then the medium was removed and

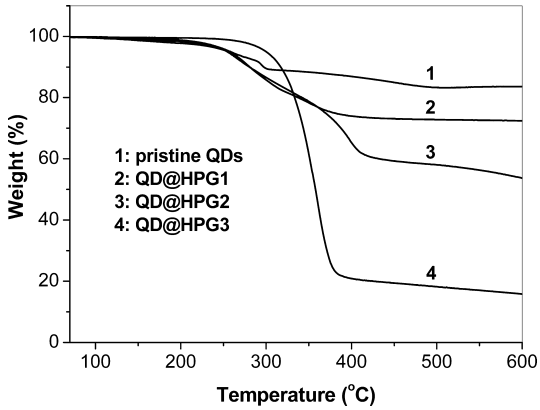


**Figure 1.** TGA weight loss curves for pristine QDs and QD@HPGs.

**Table 1.** Reaction Conditions and Selected Results for Grafting HPG from CdTe QDs Surface

| sample | $R_{wt}$[a] | $f_{wt}$[b] % | $M_n$[c] $10^{-3}$ g·mol$^{-1}$ | PDI[c] | $QY_{rd}$[d] % |
|---|---|---|---|---|---|
| QD@HPG1 | 6.7/1 | 25.7 | 8.4 | 1.69 | 15.5 |
| QD@HPG2 | 28.3/1 | 41.0 | 33.2 | 1.80 | 11.3 |
| QD@HPG3 | 61.7/1 | 80.5 | 97.8 | 1.57 | 4.5 |

[a] Weight feed ratio of glycidol/QDs. [b] The weight fraction of grafted polymer in the product of QD@HPG calculated from corresponding TGA data. [c] The number-average molecular weight ($M_n$) and polydispersity index (PDI) of the free polymer collected from the centrifugal solution, measured by GPC with DMF as the eluent and PS as the calibration. [d] Quantum yield of QD@HPG with the reference of rhodamine 6G.

150 $\mu$L of dimethylsulfoxide (DMSO) was added. The absorbance was recorded at 565 nm to assay for cell viability.

**In Vitro Imaging.** Cells A375 were cultured on coverslips, and the medium was changed every 2 days, until 85% cell confluence was achieved. Then, the pristine QDs or QD@HPG (series) probe solution was added to the cells at the concentration of 2 mg/mL. Cells were incubated at 37 °C in 5% $CO_2$ for 8 h (for comparison, much longer time such as 24 h was also studied). After incubation, the coverslips were taken out, rinsed thrice with 37 °C preheated PBS, and observed with a confocal laser-scanning fluorescence microscopy (Zeiss LSM-510) with 405 nm laser to excite the QDs.

## Results and Discussion

**Preparation and Characterization of Hyperbranched Polyglycerol-Grafted CdTe Quantum Dots.** The synthesis protocol of hyperbranched polyglycerol-grafted QDs (QD@HPG) is depicted in Scheme 1. To demonstrate the scalable fabrication of polymer-functionalized QDs, we developed the synthesis of the raw material of water-soluble CdTe QDs up to gram scale (>2 g in one batch) at first. Subsequently, the surface hydroxyl groups of as-prepared CdTe QDs were directly used to initiate the anionic ROP of glycidol, giving rise to QD@HPGs after separating the mixed ungrafted HPG by repeated centrifugation.

TGA is an effective technique to investigate the grafted HPG content on the surface of QDs. The TGA curves are shown in Figure 1. The initiating hydroxyl density of pristine QDs estimated from its 14.1% weight loss between 150−450 °C is about 2.64 mmol g$^{-1}$. Such a high density of reactive hydroxyl groups affords a good base to grow polymer from QDs by surface-initiated polymerization. Table 1 shows three selected experiments with different feed ratios of monomer to QDs. The TGA results indicate that the grafted HPG fraction ($f_{wt}$%) increases from about 25.7 to 80.5 wt % as the weight feed ratio ($R_{wt}$) rises from about 6.7:1 to 61.7:1. Correspondingly, the number-average molecular weight ($M_n$) of the free HPG also increases from 8400 to 97800. Hence, we can speculate that

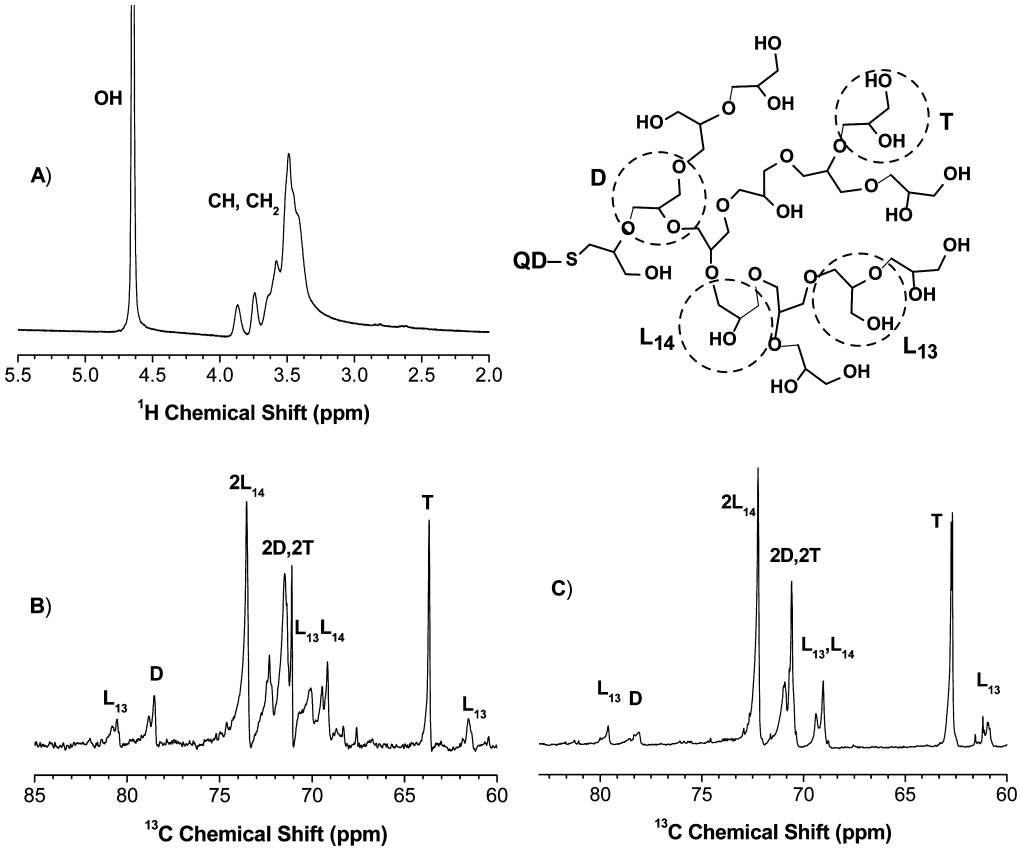


**Figure 2.** (A) $^1$H NMR spectra of QD@HPG in $D_2O$. (B) $^{13}$C inverse-gated NMR spectra of QD@HPG in $D_2O$. (C) $^{13}$C inverse-gated NMR spectra of neat HPG in $D_2O$.

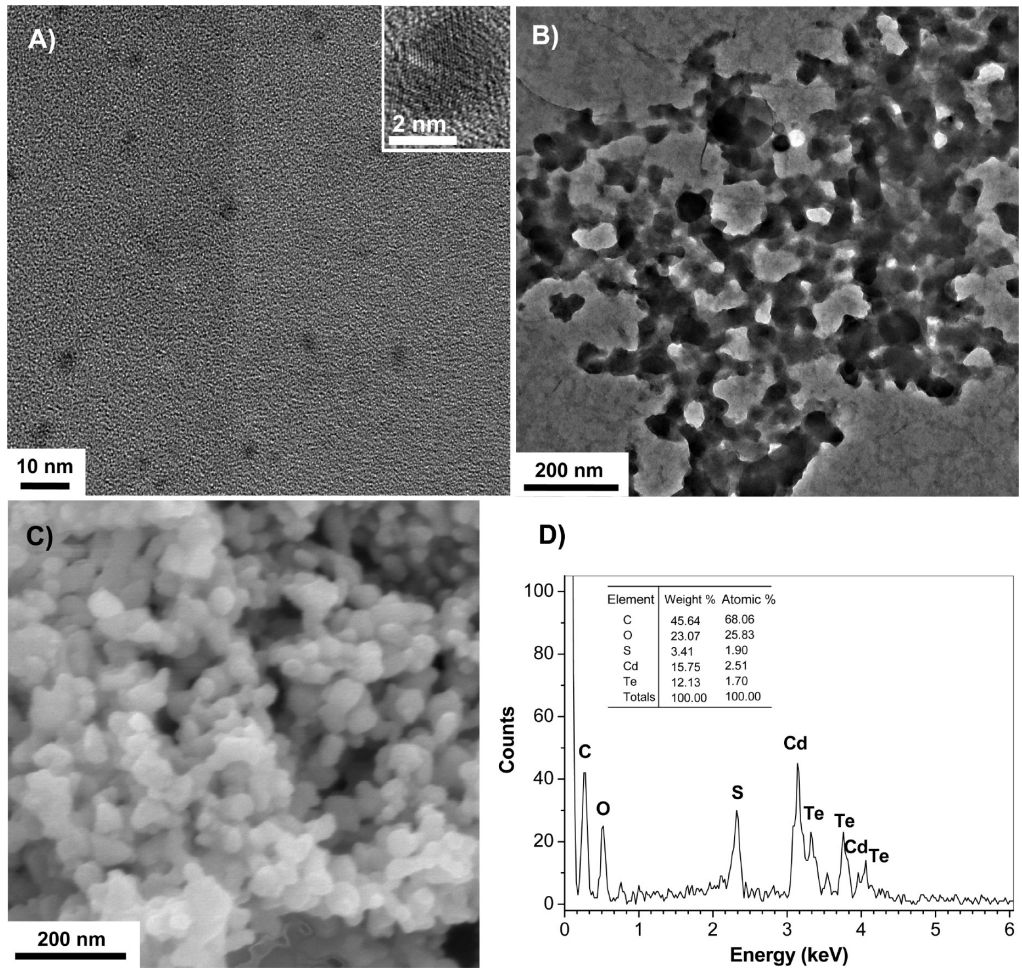


**Figure 3.** Typical TEM images of the pristine QDs (A) and QD@HPG2 (B), SEM image of QD@HPG2 (C), and EDX spectrum of QD@HPG2 (D). The inset of (A) shows the high-resolution TEM image, confirming the pristine QDs are well-crystallized.

the increase of grafted polymer fraction is attributed to the rising of molecular weight, which is in agreement with the controllable mechanism of in situ anionic polymerization.[43] It is no doubt that $f_{wt}$% can be easily adjusted through manipulating the $R_{wt}$ by such an in situ polymerization in the presence of dioxane, which is used as an emulsifying agent and dispersant.[44]

The chemical structures of CdTe@HPG were confirmed by $^{1}$H NMR and $^{13}$C inverse-gated NMR spectra (Figure 2). The inverse-gated $^{13}$C NMR spectrum of QD@HPG (Figure 2B) is quite similar to that of neat HPG (Figure 2C), suggesting both grafted and free HPG have similar dendritic structures. Furthermore, from the $^{13}$C inverse-gated NMR spectrum, the linear units of $L_{13}$ and $L_{14}$, and dendritic (D) and terminal units (T) of HPG can be assigned clearly. Accordingly, the degree of branching (DB) can be facilely calculated and for QD@HPG3 is 0.48, which is quite close to its corresponding free HPG (DB = 0.55).[45] In short, these results demonstrated that multihydroxy dendritic polymer with high DB have been successfully grafted from QDs surface.

The nanostructures and morphology of QD@HPGs were characterized by TEM, SEM, and AFM. Figure 3A and B show the representative TEM images of the pristine QDs and QD@HPG2, respectively. The pristine QDs were relatively monodisperse with the average size of 3.5 nm in diameter. The high-resolution image given in the inset shows lattice fringes, indicating that the as-prepared QDs are highly crystallized. For the QD@HPG2, the QDs are distributed evenly in the continuous HPG phase, forming QD-HPG nanohybrids with irregular sphericity. A representative SEM image of QD@HPG2 is shown in Figure 3C. The QDs are totally enveloped by HPG, no single QD phase can be observed, which is in agreement with the TEM studies. The average size of the QD@HPG2 is 35 nm, which is much bigger than the pristine QDs due to the coverage of HPG. The corresponding energy-dispersive X-ray (EDX) spectrum demonstrated the presence of Cd, Te, S, C, and O elements in the sample of QD@HPG2 (see Figure 3D). The high peaks of C and O could indicate the presence of HPGs on the surface of QDs, and the atomic ratio of C to O is close to 3:2, which is in accordance with the composition of the HPG. AFM measurements show that the QD@HPG1 can well be dispersed with irregular sphericity and relative big size (5−8 nm) compared to pristine QD (see Figure S1). This also indicates that the size of QD@HPG can be well controlled by adjusting the grafted polymer content, which is very important since only a certain size range of QD is suited in cell and in vivo applications.[46]

To further study the size and size distribution of the pristine QDs and QD@HPGs in aqueous solution at different concentrations, DLS measurements were conducted (see Figure 4). Generally, the size of pristine QDs and QD@HPGs from DLS are slightly bigger than the values obtained from the TEM and AFM measurements. This can be explained that the thiol-molecules or HPG polymers on the QDs surface are outspread in solution but highly contractive after drying on copper grids or mica surface. For pristine QDs, at low concentration (0.5 mmol/L), most of QDs were monodisperse in water, and

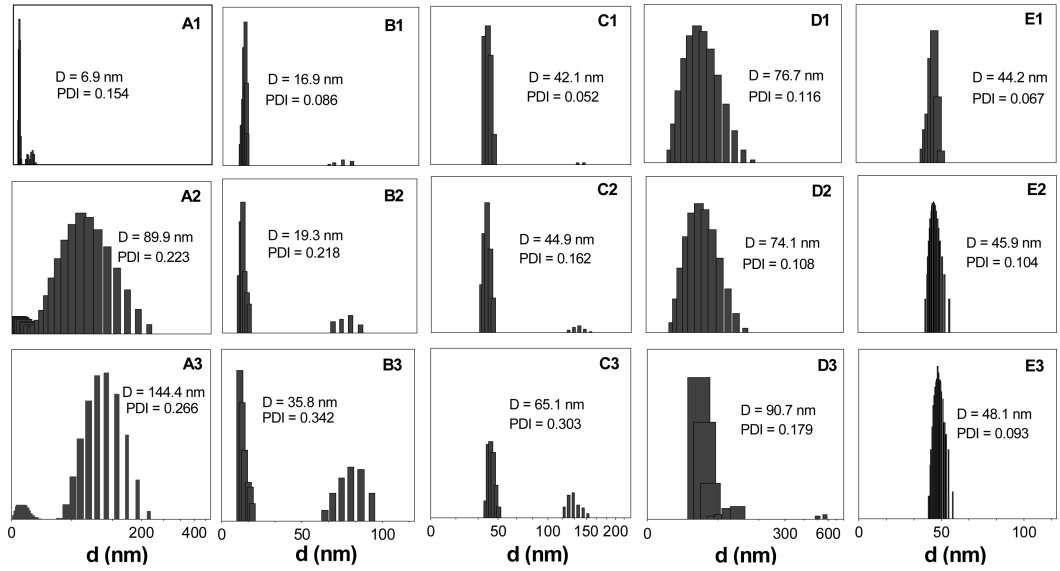


**Figure 4.** Dynamic light scattering (DLS) results of pristine QDs (A1, A2, and A3), QD@HPG1 (B1, B2, and B3), QD@HPG2 (C1, C2, and C3), QD@HPG3 (D1, D2, and D3), and QD@HPG2-Boc (E1, E2, and E3) at concentrations of 0.5 (the top row), 2.0 (the middle row), and 5.0 mmol/L (the bottom row), respectively. Samples of pristine QDs and QD@HPGs were dissolved in water, and QD@HPG2-Boc was dissolved in dichloromethane.

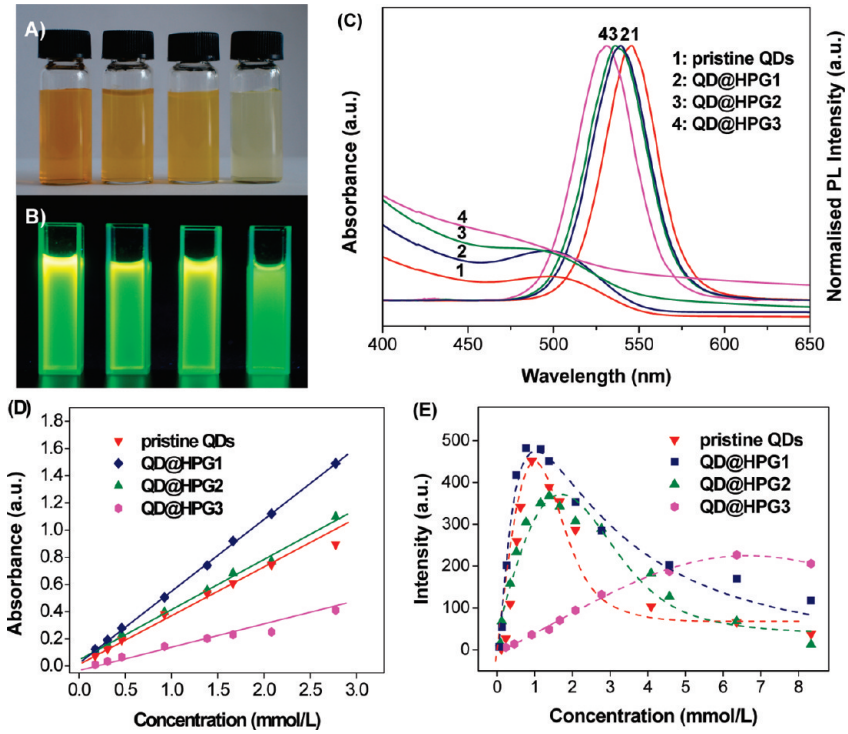


**Figure 5.** (A) Photograph of pristine CdTe QDs and QD@HPGs placed in water (from left to right: pristine QDs, QD@HPG1, QD@HPG2, QD@HPG3). (B) Photograph of aqueous samples irradiated at 365 nm (from left to right: pristine QDs, QD@HPG1, QD@HPG2, QD@HPG3). (C) Absorption and emission spectra of pristine QDs and QD@HPGs in water. Plot absorbance (D) and fluorescent intensity (E) as a function of CdTe concentration.

aggregation can be found for only small part of particles. However, as the concentrations were increased to 2.0 and 5.0 mmol/L, obvious aggregation was detected and the average diameter (*D*) of particles rose from 6.9 to 89.9 and 144.4 nm, respectively. For the QD@HPGs, the average diameter increased with the increase of grafting content of HPG, which is in accordance with the rising tendency of corresponding molecular weights of grafted HPG. At higher concentrations, QD@HPGs exhibited better monodisperse ability than pristine QDs, and the higher content of grafted HPG on QDs surface associated with the less aggregation in aqueous solution. For QD@HPG3, there is even no obvious aggregation at the highest concentration (5.0 mmol/L). This improved dispersion in aqueous solution for QD@HPGs can be ascribed to the protection of the polymer shell on the QDs surface.

After polymerization, the products of QD@HPGs are still highly soluble (Figure 5A) in water because of the hydrophilic HPG. Perhaps the most important aspect needed to be cared for the QD@HPG is whether the fluorescence of QDs was quenched or not during the preparation in such an alkaline medium. Amazingly, the resulting nanohybrids still exhibit good optical property in water (Figure 5B and Table 1). Absorption

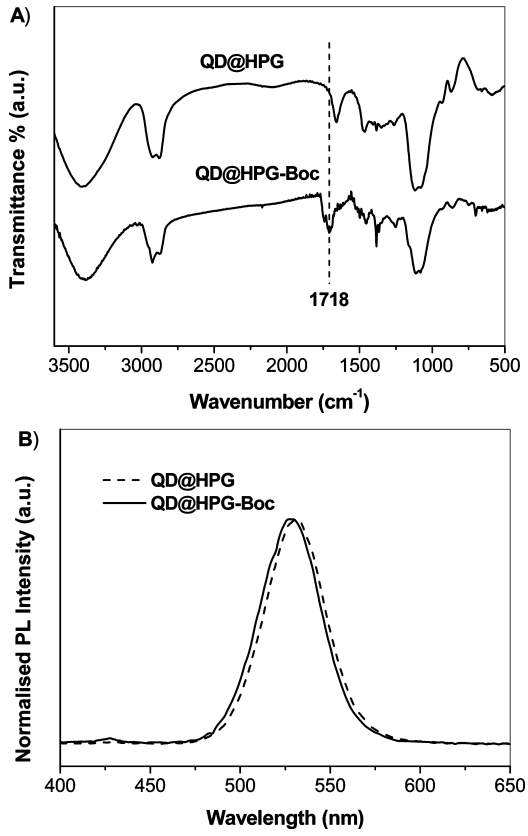


**Figure 6.** (A) FT-IR spectra of QD@HPG and QD@HPG-Boc. (B) Fluorescence spectra of QD@HPG and QD@HPG-Boc.

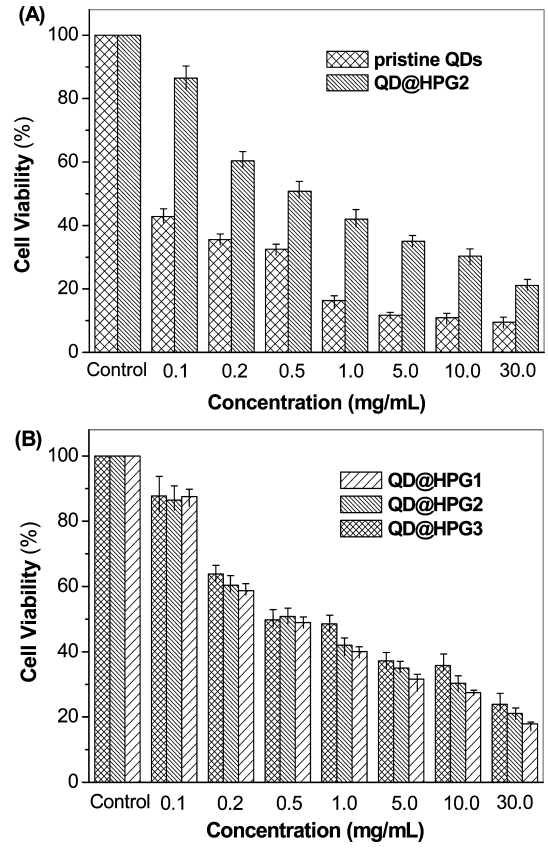


**Figure 7.** Relative cell viability of (A) pristine QDs and QD@HPG2 and (B) QD@HPGs with different concentrations obtained from human lung cancer cells SPCAI using standard MTT colorimetric assays.

and emission spectra of pristine QDs and QD@HPGs were presented in Figure 5C. With the increase of grafted polymer content, a progressive blue shift of the emission and absorption peaks of QD@HPG can be clearly viewed compared with the pristine QDs. In addition, both emission and absorption spectra become broader after the polymerization. It is generally accepted that the position and shape of the adsorption peaks are affected by the nature, size and shape of the nanoparticles. We speculated that the ROP and its resulting polymer shell have a dramatic effect on QD surface properties. First, the surface-initiated ROP reaction may slightly reduce the QDs size and as a consequence blue shift was observed. Second, with the increase of grafted HPG content, the dominant component of the QD@HPG becomes the HPG polymer that shows completely different optical properties (e.g., surface refraction index) with QDs. Third, HPGs on the surface of each QD can seal each QD in the closing loops, which further enhances the relative cumulation density of QDs compared with the pristine QDs. To further study the polymer shell effect, absorbance, and fluorescent intensity as a function of concentration were plotted in Figure 5D and E, respectively. The sample concentration was determined according to the CdTe content based on the TGA results. After the coverage of polymer, the extinction coefficients (proportional to the slope) varied obviously and higher HPG content presents smaller extinction coefficients (Figure 5D). Figure 5E shows that all the samples have a fluorescent critical concentration (FCC) and the FCC increases with the HPG content. A possible explanation for the observed decrease in PL is an autoabsorption effect, due to overlap of the PL peak with the edge of the absorption band; as the absorbance increases above a critical value with increasing particle concentration, some of the emitted light is absorbed by the particles themselves, resulting in fewer PL photons at the detector.[47] In addition, the results were in good agreement with the DLS results. On one hand, with the increase of the concentration, the QDs began to aggregate and led to the increase of the particle−particle interaction that can cause self-quenching of fluorescence. On the other hand, because the higher grafted HPG content resulted in the less aggregation or self-quenching in solution at a relatively high concentration, the FCC of the QD@HPGs increased with the grafted HPG contents.

Because various biomolecules such as proteins, amino acids, and anticancer drugs may need to be conjugated to QD surfaces, it is essential to guarantee enough functional groups on QD surfaces.[48,49] Multifunctional polymer-coated QDs were usually achieved through ligand exchange or ligand capping strategies. For example, Wisher et al.[50] synthesized a partial thiolated PAMAM dendrimer to replace the TOPO molecules on CdSe/ZnSe through ligand exchange. Duan et al.[51] prepared PEG-*g*-PEI and multidentate triblock copolymer coated QDs by ligand exchange. Parak and co-workers[52] synthesized an amphiphilic polymer based on a poly(maleic anhydride) backbone to coat the QDs directly. Herein, we reported the novel method to coat QDs with multihydroxyl HPG based on in situ ROP polymerization. As mentioned above, the QD@HPG could be a highly reactive nanoplatform for immobilizing biomolecules and drugs. To test the reactivity of the hydroxyl groups on the periphery of QD@HPG, a protected amino acid BOC-L-phenylalanine (Boc-Phe-OH) was used as a model bioreagent to couple with QD@HPG in DMF in the presence of dicyclohexylcarbodiimide (DCC). After reaction, the carbonyl absorption peak at 1718 $cm^{-1}$ appears in the FT-IR spectrum, which is in accordance with the structure of the derivative QD@HPG (Figure 6A). Interestingly, the Boc-Phe-OH functionalized QD@HPG can

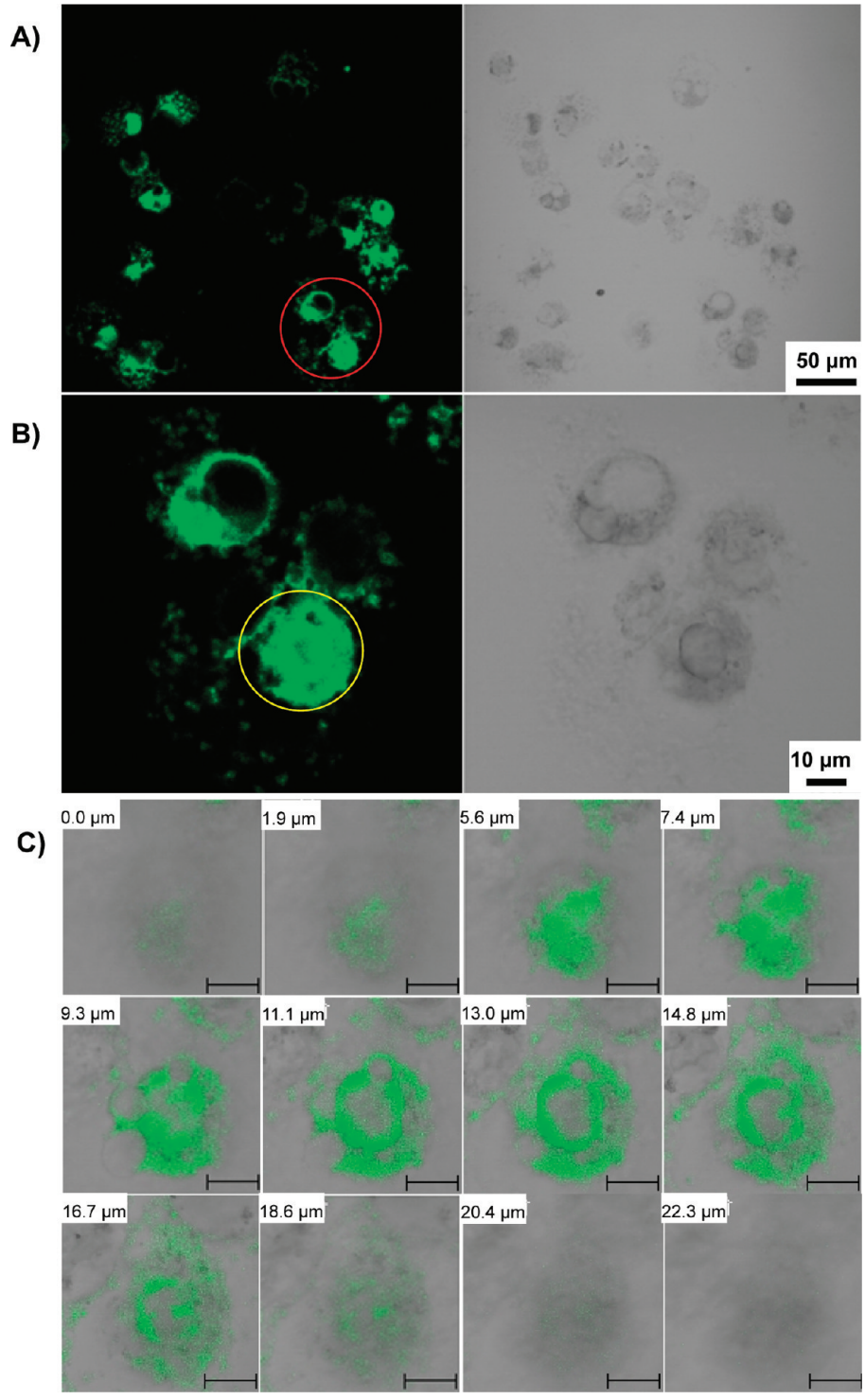


**Figure 8.** Representative confocal microscopy images of A375 cells incubated with QD@HPG2 (at 2 mg/mL for 8 h) at low (A) and high (B) magnification, and the corresponding slice scanning images (all the scale bars are 10 $\mu$m; the scanning thickness is showed at the top left corner) (C). In both A and B, the left image represents fluorescence image, the right image represents the visible image.

be well dissolved in common organic solvents such as DMF, chloroform, and dichloromethane besides in water because of the hydrophobic nature of Boc-Phe-OH, and can still emit strong fluorescence with little blue shift (Figure 6B). In addition, the distribution of the QD@HPG2-Boc in dichloromethane was also studied by DLS measurements (Figure 4) and it is found that the QD@HPG2-Boc exhibited excellent distribution in organic solution (PDI lower 0.11), and no aggregation was found at the measured concentration range (0.5−5.0 mmol/L), likely due to the protection of apolar polymer shell resulted from the DCC coupling. All these suggest that the QD@HPG is a promising candidate for lighting drug delivery.

**Preliminary Biological Evaluation.** It is well-known that two of the big challenges for application of QDs in nanobiotechnology are their toxicity and fast fluorescence bleaching.[53] Therefore, we investigated cytotoxicity and fluorescence retentivity of our functionalized QDs in cells.

It is found that the QDs surface bioactivity and oxidative extent are important factors that can determine their cellular

toxicity. Hence, as a coating material, first it had to be biocompatible itself. Various oxidation pathways especially the UV-irradiation result in forming of chalcogenoxides (e.g., $SO_2$, $SO_3$, $SeO_2$, and $TeO_2$) and free $Cd^{2+}$ ions, which make the biggest part of "contribution" to the QDs cytotoxicity.[54] Although at very low concentration (lower 0.2 mg/mL) of QDs, most reports did not find obvious adverse effects on cell viability.[55] There is no doubt that the QDs have cytotoxicity when over the safe range. Hence, we used biocompatible HPG to coat QD, and the cytotoxic experiment was carried out in a comparable high concentration region (from 0.1 to 30 mg/mL). Figure 7A shows the concentration-dependent reduction in cell viability of pristine CdTe QDs and QD@HPG2. The pristine QDs are not very toxic to human lung cancer cells SPCAI at a low concentration of 0.1 mg/mL, but the toxicity is dramatically increased when the concentration is over 1.0 mg/mL. For QD@HPG2, however, the cell viability at a concentration 1.0 mg/mL of QD@HPG remains the same level as that at a concentration 0.1 mg/mL of pristine DQs. This can be explained by the coverage of the biocompatible polymer shell. At high concentration (5.0−30.0 mg/mL), a half and even a third of the toxicity of the pristine QDs was observed for QD@HPG2. It is demonstrated that the HPG can greatly reduce the cytotoxicity of the QDs indeed. No remarkable distinction of cell viability was observed for QD@HPGs with different contents of HPG although more grafted HPG showed a tendency of less toxic to the cells (Figure 7B). This implies that the polymer clothing on QDs surface is absolutely important for lowering cytotoxicity, and the thickness of the grafted polymer layer has no considerable influence on the decrease of toxicity or the quantity of 25.7 wt % polymer is enough for protection of cells from envenomation of QDs. The results verify that strong fluorescence and low toxicity of QD@HPGs can be facilely available through the anionic ROP strategy.

To probe whether the grafted HPGs can improve the biostability of the QDs (e.g., fluorescence retentivity), we studied cell imaging for pristine QDs and QD@HPGs in cells SPCAI and A375. It is found that almost no or very weak fluorescence was observed for pristine QDs after cells SPCAI were incubated for 24 h (Figure S2A). This demonstrates that the QDs are susceptible to aggregation in biological media without the polymer clothing.[56] Hence, it is almost impossible to use the pristine QDs as fluorescent labels/probes in biology despite their good water solubility. On the contrary, strong green fluorescence retained in the case of QD@HPG2 (Figure S2B), suggesting that the QD@HPG is significantly robust in bioapplications. These also emphasize the crucial importance of polymer clothing on QDs, reducing cytotoxicity and improving fluorescence biostability at the same time. To check if the QD@HPGs can penetrate the cell wall by endocytosis, cell imaging in cells A375 was further studied by confocal laser scanning fluorescent microscopy. Figure 8A,B clearly showed that the QD@HPGs were mostly localized in the cells interior even in the cell nucleus. Slice analysis (Figure 8C) gave more believable information that QD@HPGs did not "float" on the top of cells but localized in the cells interior indeed. All these results indicate that QD@HPG is a good candidate for bioapplications. The immobilization of other biomolecules and application of the QD@HPGs in bionanotechnology are in progress and will be reported later.

## Conclusions

We report here a facile but effective strategy to functionalize water-soluble CdTe QDs with dendritic/hyperbranched polyglycerol based on in situ anionic ring-opening polymerization. The resulting QD@HPG nanohybrids are still water-soluble and show strong fluorescence. Numerous functional hydroxyl groups associated with HPG can be used to react with various functional molecules. The QD@HPGs showed much less toxicity than pristine QDs in the in vitro cytotoxicity evaluation. Also, due to the protection of the HPG on the surface of QDs from attacking of biological media, the QD@HPGs can still emit strong fluorescence in cells, while the fluorescence of pristine QDs was almost quenched. In comparison with other reported QD@polymers, our new QD@HPG nanohybrids are quite attractive for three reasons: (1) simple, efficient, and scalable synthesis strategy that combines the facile operation and low-cost reagents with good fluorescent performance of functionalized product; (2) multifunctional nanoplatform based on dendritic polyglycerol for further conjugation of other functional matters; (3) biocompatibility and fluorescence biostability due to the biocompatible polymer clothing. We believe that these fascinating QD@HPG nanomaterials have great potential in drug delivery, cell and tissue imaging, biosensors, and other biomedical applications.

**Acknowledgment.** This work was financially supported by the National Natural Science Foundation of China (No. 50773038), National Basic Research Program of China (973 Program; No. 2007CB936000), Science and Technology Commission of Shanghai Municipality (07pj14048), the Program for New Century Excellent Talents in University of China, and the Foundation for the Author of National Excellent Doctoral Dissertation of China (No. 200527).

**Supporting Information Available.** AFM images of polymer-grafted QDs, and fluorescence microscopy images of SPCAI cells incubated with QDs. This material is available free of charge via the Internet at http://pubs.acs.org.

## References and Notes

(1) Alivisatos, A. P. *Science* **1996**, *217*, 933–937.
(2) Michalet, X.; Pinaud, F. F.; Bentolila, L. A.; Tsay, J. M.; Doose, S.; Li, J. J.; Sundaresan, G.; Wu, A. M.; Gambhir, S. S.; Weiss, S. *Science* **2005**, *307*, 538–544.
(3) Lee, J.; Sundar, V. C.; Heine, J. R.; Bawendi, M. G.; Jensen, K. F. *Adv. Mater.* **2000**, *12*, 1102–1105.
(4) Raffaelle, R. P.; Castro, S. L.; Hepp, A. F.; Bailey, S. G. *Prog. Photovoltaics* **2002**, *10*, 433–439.
(5) Chan, W. C. W.; Nie, S. *Science* **1998**, *281*, 2016–2018.
(6) Medintz, I. L.; Uyeda, H. T.; Goldman, E. R.; Mattoussi, H. *Nat. Mater.* **2005**, *4*, 435–446.
(7) Murray, C. B.; Norris, D. J.; Bawendi, M. G. *J. Am. Chem. Soc.* **1993**, *115*, 8706–8715.
(8) Uyeda, H. T.; Medintz, I. L.; Jaiswal, J. K.; Simon, S. M.; Mattoussi, H. *J. Am. Chem. Soc.* **2005**, *127*, 3870–3878.
(9) Wuister, S. F.; Swart, I.; Driel, F. V.; Hickey, S. G.; Donega, C. M. *Nano Lett.* **2003**, *3*, 503–507.
(10) Wang, M.; Felorzabihi, N.; Guerin, G.; Haley, J. C.; Scholes, G. D.; Winnik, M. A. *Macromolecules* **2007**, *40*, 6377–6384.
(11) Gaponik, N.; Talapin, D. V.; Rogach, A. L.; Hoppe, K.; Shevchenko, E. V.; Kornowski, A.; Eychmüller, A.; Weller, H. *J. Phys. Chem. B* **2002**, *106*, 7177–7185.
(12) Li, L.; Qian, H.; Ren, J. *Chem. Commun.* **2005**, *5*, 528–530.
(13) Zhang, H.; Cui, Z.; Wang, Y.; Zhang, K.; Ji, X.; Lü, C.; Yang, B.; Gao, M. Y. *Adv. Mater.* **2003**, *15*, 777–780.
(14) Qian, H.; Dong, C.; Weng, J.; Ren, J. *Small* **2006**, *2*, 747–751.
(15) Derfus, A. M.; Chan, W. C. W.; Bhatia, S. N. *Nano Lett.* **2004**, *4*, 11–18.
(16) Hines, M. A.; Guyot-Sionnest, P. *J. Phys. Chem.* **1996**, *100*, 468–471.

(17) Seo, H.; Kim, S. W. *Chem. Mater.* **2007**, *19*, 2715–2717.
(18) Yang, Y.; Gao, M. *Adv. Mater.* **2005**, *17*, 2354–2357.
(19) He, Y.; Lu, H. T.; Sai, L. M.; Su, Y. Y.; Hu, M.; Fan, C. H.; Huang, W.; Wang, L. H. *Adv. Mater.* **2008**, *20*, 3416–3421.
(20) Wan, D. C.; Fu, Q.; Huang, J. L. *J. Appl. Polym. Sci.* **2006**, *102*, 3679–3684.
(21) Lemon, B. I.; Crooks, R. M. *J. Am. Chem. Soc.* **2000**, *122*, 12886–12887.
(22) Wang, C. M.; Moffitt, M. G. *Langmuir* **2004**, *20*, 11784–11796.
(23) Du, H.; Xu, G. Q.; Chin, W. S.; Huang, L.; Ji, W. *Chem. Mater.* **2002**, *14*, 4473–4479.
(24) Chen, L.; Zhu, J.; Li, Q.; Chen, S.; Wang, Y. *Eur. Polym. J.* **2007**, *43*, 4593–4601.
(25) Carrot, G.; Scholz, S. M.; Plummer, C. J. G.; Hilborn, J. G.; Hedrick, J. L. *Chem. Mater.* **1999**, *11*, 3571–3577.
(26) Lei, Y.; Tang, H.; Zhou, C.; Zhang, T.; Feng, M.; Zou, B. *J. Lumin.* **2008**, *128*, 277–281.
(27) Yu, W. W.; Chang, E.; Falkner, J. C.; Zhang, J.; Al-Somali, A. M.; Sayes, C. M.; Johns, J.; Drezek, R.; Colvin, V. L. *J. Am. Chem. Soc.* **2007**, *129*, 2871–2879.
(28) Chen, S.; Zhu, J.; Shen, Y.; Hu, C.; Chen, L. *Langmuir* **2007**, *23*, 850–854.
(29) Li, J.; Hong, X.; Liu, Y.; Li, D.; Wang, Y.; Li, J.; Bai, Y.; Li, T. *Adv. Mater.* **2005**, *17*, 163–166.
(30) Xu, J.; Wang, J.; Mitchell, M.; Mukherjee, P.; Jeffries-EL, M.; Petrich, J. W.; Lin, Z. *J. Am. Chem. Soc.* **2007**, *129*, 12828–12833.
(31) Liu, J.; Li, H.; Wang, W.; Xu, H.; Yang, X.; Liang, J.; He, Z. *Small* **2006**, *2*, 999–1002.
(32) Li, D. X.; Cui, Y.; Wang, K. W.; He, Q.; Yan, X. H.; Li, J. B. *Adv. Funct. Mater.* **2007**, *17*, 3134–3140.
(33) Joubert, M.; Delaite, C.; Bourgeat-Lami, E.; Dumas, P. *J. Polym. Sci., Part A* **2004**, *42*, 1976–1984.
(34) Ederlé, Y.; Mathis, C. *Macromolecules* **1997**, *30*, 4262–4267.
(35) Fan, Q. L.; Neoh, K. G.; Kang, E. T.; Shuter, B.; Wang, S. C. *Biomaterials* **2007**, *28*, 5426–5436.
(36) Skaff, H.; Emrick, T. *Angew. Chem., Int. Ed.* **2004**, *43*, 5383–5386.
(37) Skaff, H.; Ilker, M. F.; Coughlin, E. B.; Emrick, T. *J. Am. Chem. Soc.* **2002**, *124*, 5729–5733.
(38) Sill, K.; Emrick, T. *Chem. Mater.* **2004**, *16*, 1240–1243.
(39) Esteves, A. C. C.; Bombalski, L.; Trindade, T.; Matyjaszewski, K.; Barros-Timmons, A. *Small* **2007**, *3*, 1230–1236.
(40) Carrot, G.; Rutot-Houzé, D.; Pottier, A.; Degée, P.; Hilborn, J.; Dubois, P. *Macromolecules* **2002**, *35*, 8400–8404.
(41) (a) Kainthan, R. K.; Hester, S. R.; Levina, E.; Devine, D. V.; Brooks, D. E. *Biomaterials* **2007**, *28*, 4581–4590. (b) Kainthan, R. K.; Brooks, D. E. *Biomaterials* **2007**, *28*, 4779–4787.
(42) Liu, Y. F.; Chen, W.; Joly, A. G.; Wang, Y. Q.; Pope, C.; Zhang, Y. B.; Bovin, J. O.; Sherwood, P. *J. Phys. Chem. B* **2006**, *110*, 16992–17000.
(43) Yagci, Y.; Tasdelen, M. A. *Prog. Polym. Sci.* **2006**, *31*, 1133–1170.
(44) Kainthan, R. K.; Muliawan, E. B.; Hatzikiriakos, S. G.; Brooks, D. E. *Macromolecules* **2006**, *39*, 7708–7717.
(45) Sunder, A.; Hanselmann, R.; Frey, H.; Mü1haupt, R. *Macromolecules* **1999**, *32*, 4240–4246.
(46) Smith, A. M.; Nie, S. *J. Am. Chem. Soc.* **2008**, *130*, 11278–11279.
(47) Tekin, E.; Smith, P. J.; Hoeppener, S.; van der Berg, A. M. J.; Susha, A. S.; Rogach, A. L.; Feldmann, J.; Schubert, U. S. *Adv. Funct. Mater.* **2007**, *17*, 23–28.
(48) Hezinger, A. F. E.; Tessmar, A.; Goepferich, A. *Eur. J. Pharm. Biopharm.* **2008**, *68*, 138–152.
(49) Zheng, Y.; Yang, Z.; Li, Y.; Ying, J. Y. *Adv. Mater.* **2008**, *20*, 3410–3415.
(50) Wisher, A. C.; Bronstein, I.; Chechik, V. *Chem. Commun.* **2006**, *15*, 1637–1639.
(51) Duan, H.; Nie, S. *J. Am. Chem. Soc.* **2007**, *129*, 3333–3338.
(52) Lin, C. A. J.; Sperling, R. A.; Li, J. K.; Yang, T. Y.; Li, P. Y.; Zanella, M.; Chang, W. H.; Parak, W. J. *Small* **2008**, *4*, 334–341.
(53) Hoshino, A.; Fujioka, K.; Oku, T.; Suga, M.; Sasaki, Y. F.; Ohta, T.; Yasuhara, M.; Suzuki, K.; Yamamoto, K. *Nano Lett.* **2004**, *4*, 2163–2169.
(54) Kirchner, C.; Liedl, T.; Kudera, S.; Pellegrino, T.; Javier, A. M.; Gaub, H. E.; Stölzle, S.; Fertig, N.; Parak, W. J. *Nano Lett.* **2005**, *5*, 331–338.
(55) Su, Y.; He, Y.; Lu, H.; Sai, L.; Li, Q.; Li, W.; Wang, L.; Shen, P.; Huang, Q.; Fan, C. *Biomaterials* **2009**, *30*, 19–25.
(56) Aldana, J.; Wang, Y. A.; Peng, X. G. *J. Am. Chem. Soc.* **2001**, *123*, 8844–8850.

BM9002877